Supporting Information

Overballe-Petersen et al. 10.1073/pnas.1315278110

SI Text

SI Results

Detection and Quantification of Natural Transformation by Short and Very Short DNA. *Acinetobacter baylyi* JV28 (1) is derived from *A. baylyi* (formerly *A. cacloaceticus*) DSM588 (ADP1 *trpE27*), obtained from Deutsche Sammlung von Mikroorganismen und Zellkulturen, and carries the *trpE27* mutation rendering the strain auxotrophic for tryptophan (2). TrpE encodes anthranilate synthase subunit I, which is part of the tryptophan biosynthesis pathway. We identified the mutation by DNA sequencing as a G→A transition at position 883 of the *trpE* ORF (1,494 bp), resulting in an amino acid change (E295K; Fig. 1*A*) rendering the gene product nonfunctional. JV28 was transformable to prototrophy by DNA (100 ng/mL) of sizes ranging from ≥50 kbp down to 20 bp using purified chromosomal $trpE^+$ DNA, and PCR products and hybridized primers carrying the $trpE^+$ marker nucleotide in the center at frequencies significantly higher than the spontaneous mutation frequency (Fig. 1*C*).

Identification and Characterization of the Single-Strand–Specific Exonuclease Functions in *A. baylyi*. Previous studies indicate that absence of exonucleases specific for single-stranded DNA (ssDNA) prolongs the stability of short ssDNA molecules in the bacterial cytoplasm (3, 4). We hypothesized that prolonged stability would also be true for short DNA that enters the cytoplasm in a single-stranded form during transformation. The RecJ 5′-ssDNA-exonuclease has been characterized previously (5, 6). BLAST searches (7) of the published *A. baylyi* ADP1 genome [GenBank NC_005966 (8)] revealed an *exoX* gene (ACIAD2257; encoding the 3′-ssDNA-exonuclease ExoX), but no genes for ExoI, the subunits of ExoVII, nor other known prokaryotic or phage ssDNA exonucleases (*rnt* was not considered). We deleted the *exoX* gene in the wild type and in a Δ*recJ* strain and characterized the deletion with respect to the role of the gene product in DNA mismatch repair (MMR). It is thought that ssDNA-exonucleases degrade the erroneous-nucleotide–containing ss-fragment separated by the MMR helicase (9). Consequently, the spontaneous mutation frequency is increased in the absence of ss-exonucleases. The spontaneous mutation frequency in the Δ*recJ* Δ*exoX* strain (SI5) was increased threefold to sevenfold compared with wild type but not in the individual single mutants (Table S1). This is consistent with observations in *Escherichia coli* strains lacking the four known ss-exonuclease functions [ExoI, ExoVII, ExoX, and RecJ (9)], and indicates that RecJ and ExoX provide the main ss-exonuclease activity in *A. baylyi*.

We also tested whether the Δ*recJ* Δ*exoX* strain was cold-sensitive for growth as is its *E. coli* quadruple ss-exonuclease–deficient counterpart (9) but found that it grew wild type-like at 30 °C and below. However, a Δ*recJ* Δ*exoX* Δ*sbcCD* triple mutant (SI10) was cold-sensitive for growth at 20 °C, but displayed growth with reduced viability at 30 °C (Table S1), indicating a possible yet-unidentified role for the SbcCD exonuclease and endonuclease in DNA MMR as suggested previously in *E. coli* (10). We deleted the *mutS* gene from the Δ*recJ* Δ*exoX* Δ*sbcCD* mutant, and in the resulting strain (SI12) the cold-proficient phenotype was partially restored (Table S1). This finding is in accordance with the notion that in the absence of ss-exonucleases, nonresolvable lethal DNA intermediates are formed frequently at low temperatures during DNA MMR attempts (9, 10). Overall, the results confirm that the *exoX* gene encodes an ss-exonuclease (ExoX), and that the main cellular ss-exonucleolytic activity is provided by the *recJ* and *exoX* gene products.

Natural Transformation by Single-Strand–Specific Exonuclease Mutants of *A. baylyi*. We transformed the constructed strains by donor DNA substrates of varying lengths toward Trp^+. The results are shown in Fig. S1. The Δ*recJ* single mutant (EK4) was transformable by short DNA substrates at elevated frequencies (about 10-fold increased compared with wild type). Transformation frequencies of the Δ*exoX* strain (SI4) were not different from the wild type with the donor DNA substrates tested. The transformation frequencies of the Δ*recJ* Δ*exoX* double mutant (SI5) are shown in Fig. 1*C*. In a Δ*recA* derivative of the Δ*recJ* Δ*exoX* mutant (strain SI7), the transformation frequency with chromosomal DNA was about four orders of magnitude lower than in the $recA^+$ strains (Fig. S1). The transformation frequencies were not substantially different with shorter DNA donor substrates (down to 60 bp). Overall, this strain gave approximately constant transformation frequencies with the same amounts of DNA regardless of the size of the donor DNA.

Donor DNA Molecules Are Available for Natural Transformation Independent of DNA Concentration. We investigated whether the natural transformation frequency with donor short DNA molecules was proportional to the DNA concentration in the transformation assays by using different concentrations of the Mis-6 substrate (Fig. 4*A*) with the wild type, and of Mis-6 and Oli-60 with the Δ*recJ* Δ*exoX* strain. For comparison, chromosomal DNA was also used at various concentrations. The results are shown in Fig. S2*A* and show that the transformation frequencies of all DNA substrates are directly proportional to the concentration applied (one-hit kinetic) until a saturating concentration is reached. When calculating the ratio of transformants obtained per marker-containing molecule, the transformation frequency per molecule (transformation efficiency) in the nonsaturation range is approximately constant for each donor DNA substrate and recipient (Fig. S2*B*). The result indicates that natural transformation is a function of the absolute number of molecules available and does not depend on the DNA concentration. For the Mis-6 substrate in the wild-type strain, about 8×10^{10} molecules are required to generate a transformant under the experimental conditions. We calculated the transformation efficiencies per marker-containing molecule of the wild-type and Δ*recJ* Δ*exoX* strains for the differently sized donor DNA substrates used in Fig. 1*C*, and the results are shown in Fig. 1*B*.

We found that a DNA concentration of 100 ng/mL was below the saturation with all substrates tested and used this concentration for most experiments except when indicated otherwise.

Single-Stranded DNA Tails in Donor DNA Substrates Do Not Affect Natural Transformation by Very Short DNA. To simulate naturally occurring donor DNA substrates with ssDNA tails, we prepared a set of substrates with 5′- or 3′-recessed ends (17–19 terminal nt missing of the 60-bp substrate Oli-60) in the top or bottom strand (termed Tail-1 to Tail-4; Fig. S3*A* and Fig. 2*A*). The transformation frequencies of Δ*recJ* Δ*exoX* strain with these DNA substrates are shown in Fig. S3*B* and indicate that single-stranded tails have no influence on transformation. Taken together, nicks, short gaps (see main text) or single-strand overhangs have little influence on transformation by very short DNA.

Heterologous Ends of Donor DNA or Modified 5′-Termini Do Not Affect Natural Transformation. To test the effect of heterologous DNA ends on transformation, we used a set of 60-bp donor DNA

preparations based on the 40-bp substrate (Oli-40) that contained an additional 20 heterologous base pairs at either end (Flap-1 and Flap-2; Fig. S3*A* and Fig. 2*A*). With respect to the transforming bottom strand (see main text), Flap-1 contained a heterologous 3′-tail, and Flap-2, a heterologous 5′-tail. The transformation frequencies using the Δ*recJ* Δ*exoX* strain as recipient (Fig. S3*B*) were overall not different from those of the 60- and 40-bp substrates. As comparison, we used a set of donor substrates that contained homologous tails instead of heterologous DNA (carrying the marker nucleotide base pair in asymmetric positions; Asym-1 and Asym-2; Fig. S3*A*). As shown in Fig. S3*B*, the transformation frequencies were not different from the Flap-1 or Flap-2 substrates with the Δ*recJ* Δ*exoX* strain as recipient, suggesting that heterologous 5′-ends do not interfere with recombination with very short donor DNA.

We confirmed the results by using Oli-60 derivatives that carried chemical modifications at the 5′-ends (carboxy-X-rhodamine, Fig. 2*A*; 6′-amino-hexyl-phosphate, and 12′-amino-dodecyl-phosphate; named ROX-1, C6, and C12, respectively). We also used a 60-bp substrate with phosphorylated 5′-ends (60P) that does not require processing and hypothetically can be directly joined to a 3′-OH-end by a DNA ligase after hybridization. Natural transformation of the Δ*recJ* Δ*exoX* strain by these substrates gave transformation frequencies in the same range as the Oli-60 (Fig. 2*B* and Fig. S3*B*). These findings indicate that besides endonucleolytic processing of 3′-ends during uptake, 5′-ends are also processed either exonucleolytically or endonucleolytically in the transformation process. Therefore, chemical modifications to the 3′- and 5′-ends of DNA fragments do not prevent them from serving as substrates for recombination.

Deaminated or Hydrolyzed Bases in Donor DNA Affect Natural Transformation Only When Immediately Adjacent to the Marker and Are Repaired by Base Excision Repair. The transformation frequencies of the Δ*recJ* Δ*exoX* strain by different uracil- or AP-containing 60-bp substrates (Fig. 2*A*) are shown in Fig. 2*B*. We determined the DNA sequences of randomly picked transformants obtained with Ura-4 ($n = 20$) and AP-10 ($n = 20$) substrates and found in all cases that at the lesion positions the sequence of wild-type *trpE*$^+$ was present.

With the AP-7 substrate, which contained no marker base, the frequency was about 10-fold higher than the spontaneous mutation frequency. This finding is in agreement with earlier observations that AP sites are mutagenic when not repaired (11). Uracil residues and AP sites in dsDNA are repaired by base excision repair (BER) (12). A key step in BER is nicking the DNA strand immediately 5′ of the lesion by an AP lyase (12). In the genome of *A. baylyi* (8), we identified one gene homologous to the *nth* gene of *E. coli* (ACIAD1108, encoding the AP lyase endonuclease III) using BLAST (7), but no genes for endonuclease IV or other putative bacterial AP lyases. We deleted the *nth* gene in the Δ*recJ* Δ*exoX* strain and determined transformation frequencies of this strain (KOM146) with selected uracil- and AP-containing substrates (Fig. 2 *B* and *C*). With chromosomal DNA or the 1,494-bp substrate, the transformation frequencies were not different from the SI5 strain. DNA sequencing revealed that from 20 randomly picked KOM146 transformants obtained with Ura-4, four transformants carried C→T transitions at the uracil residue position 5′ of the marker (bottom strand). As expected, no changes were found at the 3′-located uracil position, as the recipient already carried a T there. From 25 KOM146 transformants with AP-10, 10 T→A transversions at the 3′-lesion and seven C->A transversions at the 5′-lesion (bottom strand) were identified. In 15 KOM146 transformants with AP-9, 14 carried T→A transversions replacing the AP site in the donor DNA. The results suggest that BER removes lesions like uracil residues and AP sites in dsDNA after hybridization and repairs them using the complementary strand as template. When attacking the lesion directly adjacent to the marker nucleotide, BER prevents integration of that marker, presumably by the endonuclease function of the AP lyase and an inability of the gap repair functions to tolerate the mismatched marker nucleotide. In the Δ*recJ* Δ*exoX* mutant, the 100-fold decrease with AP-7 compared with Oli-60 suggests that about 1% of the lesions escape BER. In the absence of BER, lesion-containing DNA is integrated efficiently, but the lesions can cause mutations at these positions, often replacing the damaged residue with adenine.

Construction of an *A. baylyi* Strain Transformable by Mammoth Mitochondrial DNA. We decided to use DNA from an ancient source in a natural transformation experiment. Because ancient bacterial DNA is extremely difficult to authenticate, we chose to use DNA from an extinct animal. We isolated DNA from a 43,000-y-old mammoth (*Mammuthus primigenius*) bone [42,960 + 1,990/−1,600 (13)] that has been recovered from permafrost and that was part of the collection of the Centre for Geogenetics (Copenhagen, Denmark). Measurements on previous DNA extracts from that bone indicated a content of ∼250 ng total DNA per g bone matter, of which, when shot-gun sequenced, 0.05% of the reads could be mapped to *M. primigenius* mitochondrial DNA (mtDNA) (16,449 bp) with an average DNA length around 60–80 bp.

We constructed an *A. baylyi* Δ*recJ* Δ*exoX trpE*$^+$ recipient with a chromosomally located 213-bp insert as homologous anchor for recombination with mammoth mtDNA. This insert was identical to an internal segment (71 sense codons with the standard bacterial genetic code) from the mitochondrial ND5 gene, with the exception of two exchanged nucleotides at positions 90 and 91 (Fig. 2*D*) creating a double-nucleotide variant (DNV) marker. This exchange resulted in two consecutive stop codons. The insert was de novo synthesized and inserted in frame into the *hisC* gene of *A. baylyi* immediately downstream of the start codon. The resulting *hisC*::′ND5i′ allele rendered the *A. baylyi* strain (KOM218) auxotrophic for histidine. Transformability of KOM218 to prototrophy was confirmed using a 60-bp dsDNA substrate with the wild-type mammoth DNA sequence (ND5PLUS; Fig. 2*D*) in a laboratory of the Centre for Geogenetics (Copenhagen, Denmark). The replacement of the stop codons by the wild-type sense codons resulted in a functional *hisC*::ND5$^+$ allele. The transformation frequency with 100 ng/mL was $7.9 \pm 3.0 \times 10^{-6}$ ($n = 2$), which was comparable to results obtained with Mis-6 using the Δ*recJ* Δ*exoX* recipient ($5.7 \pm 2.3 \times 10^{-6}$; Fig. 4*B*) and confirmed that ND5PLUS was not attacked by MMR (see main text). The spontaneous His$^+$ mutation frequency was $8.9 \pm 11.1 \times 10^{-10}$ (see section below for description of mutants).

Natural Transformation of *A. baylyi* by 43,000-y-Old DNA. To avoid DNA contamination, the ancient DNA isolation and transformation experiments were performed in laboratories of the University of Tromsø (Norway), which are more than 1,500 km away from Copenhagen. Neither the ND5PLUS donor DNA substrate nor the respective primers were ever present in the Tromsø facilities. Total DNA was isolated from 840 g of bone material and used for natural transformation of KOM218 (1.3 L of bacterial culture, about 3.2×10^{11} cells plated on selective media). A total of 349 His$^+$ colonies were obtained. To distinguish possible recombination events with the ancient mtDNA from random mutants, we screened the isolates by PCR specific for a single wild-type nucleotide at the DNV marker. From PCR-positive isolates, the recombinant ND5 region was characterized by DNA sequencing, and we identified a single His$^+$ isolate (termed isolate 214.1) that had both recipient-specific marker nucleotides replaced by those of the wild-type mammoth mtDNA allele while the rest of the ND5-insert sequence was unaltered.

In a negative control experiment without donor DNA (2 L of culture, $\sim 1.1 \times 10^{12}$ recipient cells plated) a total of 1,573 His$^+$

colonies were recovered. All isolates were negative in the PCR screening. We randomly picked 96 colonies from the control experiment and 20 colonies from the mammoth DNA experiment and determined the recombinant *hisC* region by DNA sequencing. Three groups of mutants were identified. The first group carried in-frame deletions in the ′ND5i′-segment removing the stop codons. In >90% of the isolates from this group, the recombinant joints occurred at microhomologies (14). In the second group, small stretches (8–60 bp) covering the stop-codon DNV were substituted with unrelated chromosomal segments of similar or the same size through recombination occurring at microhomologies on both ends, rendering this group a set of illegitimate intragenomic recombinants. A small number of isolates (group three) acquired novel putative start codons including suitable ribosome binding sites downstream of the double stop codon marker, either by a single point mutation or by an illegitimate intramolecular substitution similar to those of the second group. No point mutants were discovered among the His^+ isolates that had one, or both, stop codon marker nucleotides of KOM218 altered.

The mammoth bone has been handled by humans since its recovery from permafrost. The human mtDNA ND5 allele is 74% similar to the mammoth ND5 allele over a 1,253-bp stretch. As a control experiment, we designed a 60-bp dsDNA substrate (termed ND5hum) covering the corresponding region of the human ND5 gene (Fig. 2*C*). Although the two marker nucleotides are identical in human and mammoth mtDNA, the human ND5 version contains 12 SNPs in the 60-bp stretch, among them a SNP 1 nt away from the marker DNV, generating a 4-nt loop (Fig. 2*D*). To assess whether contaminating human DNA can lead to false-positive transformants, we used ND5hum substrate to transform the KOM218 strain and found that the transformation frequency ($1.1 \pm 0.5 \times 10^{-8}$) was significantly higher (*t* test; $P < 0.01$) than the mutation frequency. PCR screening revealed that the majority of His^+ isolates gave bands of the expected size. We determined the recombinant *hisC* region from 42 PCR-positive isolates by DNA sequencing. These isolates were transformants that contained both wild-type nucleotides at the marker site and also always human SNPs to various extents. Notably, in all of the 42 cases, the SNP located 2 bp away from the selective marker nucleotide pair had been cotransformed with the marker nucleotides. Consequently, natural transformation of KOM218 by human mtDNA results in transformants that acquire at least one human-specific nucleotide. Taken together, the results support the conclusion that the His^+ isolate 214.1 was neither generated by mutation nor by transformation with contaminating contemporary DNA, and is a transformant formed by 43,000-y-old DNA.

Natural Transformation by Very Short DNA Is Not Inhibited by Competing DNA. We tested whether competing donor DNA in excess amounts would interfere with uptake and recombination of very short donor DNA during transformation. Mixtures of Oli-60 with heterologous high-molecular (salmon sperm) DNA, or with a heterologous 60-bp DNA substrate (COX3hum), were used in ratios from 1:10; 1:100; and 1:1,000 as donor DNA in transformation experiments of the Δ*recJ* Δ*exoX* strain. The transformation efficiencies (calculated as transformants per marker-containing DNA molecule) were unaffected by the heterologous DNA, even when present in 1,000-fold excess (Fig. S4). To assess whether homologous competing DNA can interfere with the ssDNA-hybridization or recombination and in this way alter transformation frequencies, we used a nontransforming 60-bp DNA substrate termed TrpEminus containing the markerless *trpE27* sequence in transformation experiments. The results (Fig. S4) demonstrate that even excess of homologous but marker-free donor DNA substrates do not influence the transformation frequency of *A. baylyi*. No transformants exceeding the background mutation frequency were observed with either of the competing DNA substrates in control experiments without Oli-60.

Natural Transformation by Very Short dsDNA and ssDNA Depends on Active DNA Uptake. To examine whether short donor dsDNA or ssDNA substrates are taken up and transferred into the cytoplasm by the same cellular DNA uptake machinery as high-molecular DNA, we inactivated genes previously determined to be essential for natural transformation by chromosomal DNA. We deleted an array of genes involved in type IV pilus formation [(*comB-comF*)::*dhfr* (15)] from the Δ*recJ* Δ*exoX* strain and found that transformation frequencies of the resulting mutant KOM131 by chromosomal DNA [$(7.5 \pm 4.0) \times 10^{-11}$], by very short dsDNA [Oli-60; $(1.9 \pm 0.2) \times 10^{-10}$], and by very short ssDNA [R10; Fig. 3*B*; $(1.0 \pm 1.0) \times 10^{-10}$], were indistinguishable from the mutational background determined in control experiments without DNA [$(1.2 \pm 1.0) \times 10^{-10}$]. We also deleted the *comA* gene encoding the cytoplasmic membrane pore essential in translocation of DNA into the cytoplasm (16) from the Δ*recJ* Δ*exoX* strain and determined in a corresponding set of experiments with the resulting mutant KOM156 that transformation by chromosomal DNA [$(1.8 \pm 1.7) \times 10^{-10}$], by Oli-60 [$(1.6 \pm 0.3) \times 10^{-10}$], and by R10 [$(1.6 \pm 0.3) \times 10^{-10}$], were not different from the mutational background [$(2.0 \pm 1.0) \times 10^{-10}$]. The results show that very short DNA is taken up by the same mechanism required for uptake of larger DNA fragments through natural transformation.

Single but Not Double Adjacent Nucleotide Exchanges Are Removed by DNA MMR. The effects of the cellular MMR on donor DNA substrates containing single or multiple isolated mismatches, or two neighboring mismatches, using the Δ*recJ* Δ*exoX* strain, a mismatch repair-deficient Δ*recJ* Δ*exoX* Δ*mutS* mutant (KOM171), and the wild type as recipients, are shown in Fig. 4*B*. The results indicate that multiple adjacent mismatches escape MMR, whereas single mismatches are effectively recognized by the MMR, leading to abortion of the transformation event. DNA sequencing of 40 Δ*recJ* Δ*exoX* Δ*mutS* transformants obtained with Mis-1 (resulting in three mismatches; Fig. 4*A*) showed that the 3′-located nucleotide variations of the bottom strand have been acquired in 14 cases, and the 5′-nucleotide variations in 24 cases. Eight transformants contained only the marker nucleotide but no further nucleotide variations, indicating that in 20% of the transformants the DNA stretch integrated was ≤14 nt. These results show that MMR removes about 97% or more of all transformation attempts when a mismatch is formed, and reduces frequencies even more when multiple isolated mismatches occur. However, adjacent mismatches are not the primary target for MMR (17–19) and remain in the genome at high frequencies.

SI Materials and Methods

Construction of Bacterial Strains. Table S5 contains a list of strains used in this study and plasmids used for construction of the strains. Primers are listed in Table S4. The plasmid construction steps were confirmed by restriction analysis. The *A. baylyi* construction mutants were verified by PCR, and cointegration of plasmids was ruled out by sensitivity to antibiotic resistance genes from the plasmid backbone (usually ampicillin or chloramphenicol). In some cases, constructs were also confirmed by DNA sequencing.

The marker-free *exoX* deletions in strains SI4 and SI5 were generated according to a two-step natural transformation procedure described previously (5, 6). A 1,055-bp segment upstream of the *exoX* gene of *A. baylyi* was PCR amplified from the *A. baylyi* chromosome using the Phusion proofreading polymerase [Finnzymes (5)] and the primers exoX-up-f and exoX-up-r (carrying a heterologous 5′-tail containing an XbaI restriction site) and cloned into the OliI site of plasmid vector pGT41 (5) (Table S5) upstream of the selective/counterselective marker pair *nptII*

(kanamycin resistance) and *sacB* (susceptibility against 50 g/L sucrose). The resulting plasmid was termed pSA1. Next, a 989-bp segment downstream of *exoX* was PCR amplified using primers exoX-down-f (including a 5′-XbaI-extension) and exoX-down-r and inserted into the KspAI site of pSA1 downstream of *nptII sacB*. The resulting plasmid pSA2 carried a Δ*exoX*::(*nptII sacB*) deletion allele, embedded into its natural flanking regions. From pSA2, the *nptII sacB* genes were removed by cleavage with XbaI and circularization of the remaining fragment. This step resulted in directly fusing the cloned segments and producing a marker-free deletion allele. The resulting plasmid was named pSA3. The *A. baylyi* strain JV28 was naturally transformed by XhoI-linearized pSA2 DNA. The resulting kanamycin-resistant (and sucrose-sensitive) strain carried the Δ*exoX*::(*nptII sacB*) allele and was termed SI2. SI2 was subsequently transformed by XhoI-linearized pSA3 DNA, yielding the sucrose-resistant (and kanamycin-sensitive) strain SI4, which carried the Δ*exoX* deletion allele (verified by PCR). Correspondingly, strain EK4 (Δ*recJ*) was transformed by linearized pSA2, giving strain SI3 [Δ*recJ* Δ*exoX*::(*nptII sacB*)], and SI3 transformed by linearized pSA3 gave strain SI5 (Δ*recJ* Δ*exoX*).

From SI5, the *sbcCD* operon was deleted with a corresponding procedure sequentially using the XhoI-linearized plasmids pKH80 [generating strain SI8 carrying a Δ*sbcCD*::(*nptII sacB*) allele] and pKH81 [resulting in strain SI10 with a *sbcCD* deletion (20)].

Additional pGT41-based plasmid derivatives were constructed in this study for the chromosomal deletions of *nth* and *mutS*, and for the substitution of *comA* by the *nptII sacB* cassette. For Δ*nth*, downstream (850 bp; nth-down-f/nth-down-r) and upstream (1,092 bp; nth-up-f/nth-up-r) segments of this gene were PCR amplified and in consecutive steps inserted into pGT41, giving the plasmids pKH121 and pKH122, respectively. From pKH122, the *nptII sacB* gene cassette was removed by XbaI cleavage, giving pKH123. For Δ*mutS*, a corresponding set of plasmids was constructed by sequentially inserting downstream (401 bp; mutS-down-f/mutS-down-r3) and upstream (1,012 bp; mutS-up-f/mutS-up-r) segments of *mutS* into pGT41, giving pKH127 and pKH128, respectively. From the latter plasmid, the *nptII sacB* genes were excised (in this case with SacI), and the resulting circularized fragment was termed pKH129. For the substitution of *comA*, segments upstream (1,064 bp; comA-up-f/comA-up-r) and overlapping with the 3′-terminus (306 bp; comA-down-f3/comA-down-r3) of *comA* were PCR amplified and inserted into pGT41 in subsequent steps, giving pKHNH1 and pKHNH2, respectively. pKH122, pKH128, and pKHNH2 (all XhoI-linearized) were used to cross the respective substitution alleles into strain SI5, giving the strains KOM144 [Δ*recJ* Δ*exoX* Δ*nth*::(*nptII sacB*)], KOM168 [Δ*recJ* Δ*exoX* Δ*mutS*::(*nptII sacB*)], and KOM156 [Δ*recJ* Δ*exoX* Δ*comA*::(*nptII sacB*)], respectively. The *nth* and *mutS* deletion mutants were obtained through transformation by the respective deletion plasmids pKH123 and pKH129 (both XhoI-linearized), giving the strains KOM146 (Δ*recJ* Δ*exoX* Δ*nth*) and KOM171 (Δ*recJ* Δ*exoX* Δ*mutS*). The deletion of *mutS* in the mutator strain KOM171 was confirmed by sequencing.

From SI10, the *mutS* gene was substituted by a kanamycin resistance gene through transformation by ScaI-linearized pmutS-Ac3 (20), and the resulting strain (Δ*recJ* Δ*exoX* Δ*sbcCD* Δ*mutS*::*nptII*) was named SI12.

The *recA* mutant strains were constructed as follows: A 1,454-bp PCR product of the *recA* gene and its surrounding regions was amplified using the primers recA-Ac-f and recA-Ac-r and cloned into the EcoRV site of pBluescript II SK(+) (Stratagene), yielding the plasmid precA-Ac2. A PCR product covering the *tetA* (tetracycline resistance) gene from pRK415 (21), obtained with primers tetA-r and tetR-r, was inserted into the SnaBI site of precA-Ac2, disrupting *recA* and giving the plasmid precA-Ac4. Next, the 5′-terminal 570 bp of *recA* (and the 53 3′-terminal bp of the upstream located *hslR*) were removed by cleavage of precA-Ac4 with PmeI and EcoNI, blunting with T4 DNA polymerase, and circularization of the vector fragment, giving precA-Ac5. This plasmid was linearized by DraI and used to naturally transform the DSM588 strain, giving the tetracycline-resistant strain JV33 (Δ*recA*::*tetA*). Low concentrations of chromosomal DNA from JV33 were used to transform JV28 (resulting in strain JV37) and SI5 (resulting in strain SI7), respectively. The strain KOM131 was obtained by introducing the (*comB-comF*)::*dhfr* allele [replacement of the *comB*; ACIAD3317 (putative *pilX*); *comC*; *comE*; and *comF* genes, which are essential for type IV pilus-mediated DNA uptake, by a trimethoprim resistance gene (15, 22)] from *A. baylyi* ADP1200-2 DHFR (P. J. Johnsen) into the strain SI5. For JV37, SI7, and KOM131, cotransformation of unwanted DNA was ruled out by phenotypic tests (tryptophan auxotrophy; rifampicin resistance; inability to use hexadecane; kanamycin sensitivity) or by PCR analysis (Δ*recJ*, Δ*exoX*).

The *hisC*::′ND5i′ fusion allele was constructed as follows: First, a 213-bp DNA segment was synthesized by de novo gene synthesis (Eurofins). This segment was identical to an internal fragment of the ND5 gene (encoding subunit V of the mitochondrial NADH dehydrogenase) from clade II mammoth mitochondrion (nucleotides 12,359–12,571 from GenBank EU153450), with exception at positions 90 and 91 (Fig. 2*D*). The nucleotide exchanges at these loci resulted in forming two consecutive stop codons, which interrupt the stretch of 71 sense codons (standard bacterial genetic code) in the wild-type ND5 segment. The de novo-synthesized DNA segment was termed ′ND5i′ (“i” denoting the internal nucleotide exchanges) and was obtained as insert in a pCR2.1 plasmid vector (pCR2.1-ND5i). From this vector, the ′ND5i′ segment was recovered by cleavage with SapI and BsaI and agarose gel purification.

Second, a set of plasmid vectors were constructed as follows: A 1,139-bp segment containing the upstream region and the 5′-terminal part of *hisC*, with the start codon of *hisC* approximately in the center, was PCR amplified from the *A. baylyi* chromosome with the primers hisC-ins-f and hisC-ins-r and cloned into the HincII site of pUC19, giving pKHhisC1. Next, a segment termed SSB5 containing restriction sites for SapI, SacI, and BsaI, and a set of five linker codons coding for SerGlySerGlySer was inserted between the start codon and the second codon of *hisC* by inverse PCR using primers with suitable 5′-extensions (hisC-out-1 and hisC-out-2). The resulting plasmid was termed pKHhisC2. The cloned segment including the SSB5 modifications was excised from pKHhisC2 as BamHI/SalI fragment and inserted into the BamHI and SalI sites of pACYC184 (disrupting the tetracycline resistance gene in that plasmid). The resulting plasmid pKHhisC19 carried singular restriction sites for each SapI, SacI, and BsaI. An *nptII sacB* cassette was obtained as a SacI fragment from plasmid pKH128 and inserted into the SacI site of pKHhisC19, giving pKHhisC20 in which the upstream region and start codon of *hisC* were separated from the rest of the gene by the *nptII sacB* insertion. Finally, the ′ND5i′ SapI/BsaI fragment was inserted into the SapI and BsaI sites of pKHhisC19, resulting in a construct that had fused the ′ND5i′ in frame downstream of the start codon, and upstream of the five-codon linker and the remainder of the *hisC* fragment. The plasmid was termed pKHhisC25. The desired DNA sequence of the fusion allele (Fig. 2*D*) was confirmed by DNA sequencing.

To construct the recipient strain for transformation by mammoth mtDNA (KOM218), the SI5 strain was rendered tryptophan-prototrophic through transformation by Oli-60. The resulting strain (KOM188) was transformed by ScaI-linearized pKHhisC20, giving strain KOM213 that replaced the *hisC*$^{+}$ by the *hisC*::(*nptII sacB*) allele. Finally, KOM213 was transformed by ScaI-linearized pKHhisC25, allowing positive selection for sucrose-resistant transformants carrying the *hisC*::′ND5i′ construct. DNA sequencing confirmed the desired sequence of the entire allele, and KOM218 (like KOM213) was confirmed to be auxotrophic for histidine.

The cloning steps were carried out with standard procedures (23) using the *Escherichia coli* strains DH5α (24), SF8 *recA* (25), or EC100 (Epicentre) as hosts. If applicable, antibiotics were added at the following concentrations: ampicillin, 50 μg/mL; chloramphenicol, 10 μg/mL; kanamycin, 10 μg/mL; rifampicin, 10 μg/mL; tetracycline, 5 μg/mL; trimethoprim, 170 μg/mL. *A. baylyi* was grown on LB plates or in LB broth (BD) at 30 °C. The selective medium for prototrophic isolates in transformation experiments was M9 minimal medium (23) with 10 mM succinate (pH 7.5). In some control experiments, M9 was supplemented with tryptophan (50 mg/L) or histidine (100 mg/L).

Preparation of Donor DNA. Chromosomal DNA was prepared according to the Genomic DNA Purification protocol (Qiagen). PCR products covering the marker nucleotide of $trpE^+$ at position 883 were amplified at various sizes [1,494 (entire ORF); 700; 400; 200; 120; 100; and 80 bp (carrying the marker in the center position)] using Taq polymerase (Molzym; Finnyzmes; or Thermo Scientific) and $trpE^+$ DNA as template, and purified with the PCR Purification procedure (Qiagen). Shorter donor DNA substrates (80; 60; 40; 30; and 20 bp), and dsDNA substrates carrying ss-overhangs, 5′-adducts, uracil residues, or AP sites, were prepared by annealing complementary ssDNA primers as follows. Individual primers were diluted in a buffer containing 10 mM NaCl, 10 mM $MgCl_2$, and 10 mM Tris·HCl (pH 8.0). Complementary primers were mixed at equimolar concentrations (~100 ng/μL) and annealed in a thermocycler as follows: denaturation at 94 °C for 1 min and decrease of temperature in 1 °C steps (6 s per step) down to 40 °C. Salmon sperm DNA was from Sigma-Aldrich and dissolved in TE buffer. The DNA concentrations of all donor DNA preparations (in the case of annealed primers to adjust for the hypochromic effect of dsDNA) were determined using a NanoDrop 3300 fluorospectrometer and verified by agarose gel electrophoresis. The 80-bp DNA was prepared both as PCR and as hybridization product: no difference in transformation frequency was observed (*t* test; $P = 0.83$), and the data were pooled.

DNA from a 43,000-y old mammoth bone (13) was isolated as follows. A large piece of mammoth bone was cleaned from marrow remnants and dirt and crushed into small pieces (diameter, ~1 cm). A total of 840 g of bone pieces was recovered and ground to a fine powder in a planetary ball mill (Pulverisette 5; Fritsch) at 150 rounds per minute for 30 min. The bone powder was suspended in 1 L of EDTA (0.5 M, pH 8.0), resulting in a final volume of about 1.5 L. Twenty milliliters of *N*-laurylsarcosine (250 g/L), 15 mL of DTT (1 M), and 1 g of proteinase K were added, and the suspension was stirred at 50–55 °C for 66 h with additional amendments of 10 mL of DTT (1 M) and 0.5 g of proteinase K after 16 h, and a further 1 g of proteinase K after 40 h. Next, the suspension was centrifuged at 10,000 × *g* and 4 °C for 30 min, and the supernatant recovered (570 mL) and distributed into four Spectra/Por 1 dialysis bags (maximal volume, 400 mL) with 6- to 8-kDa exclusion size (Spectrum Europe). The lysate was dialyzed for 70 h against 20 L of dialysis buffer [1× M9 salts (23)] with buffer changes after 6, 20, 29, 45, and 52 h. The volume increased during dialysis to 1.32 L.

Natural Transformation Assays. Competent cells were prepared as follows: A freshly prepared overnight culture was diluted 1:100 in LB and aerated at 30 °C until a titer of 1×10^9 mL^{-1} was reached. The cells were chilled, sedimented at 5,000 × *g* and 4 °C for 10 min and resuspended in 0.1 vol of prechilled LB with 20% (vol/vol) glycerol. Cells were aliquoted and stored at −80 °C until use. For transformation, competent cells were thawed on ice and diluted 1:40 in LB (assay titer: 2.5×10^8 cells·mL^{-1}). Donor DNA was added to a final concentration of 100 ng/mL, unless otherwise indicated. For transformation by mammoth DNA, the raw dialysate (for control experiments: dialysis buffer) was amended with 10 g/L tryptone and 5 g/L yeast extract (both BD) before competent cells were added (assay titer: 2.5×10^8 cells·mL^{-1}). The assays were aerated for 90 min at 30 °C, washed, and resuspended in PBS (23), and plated in appropriate dilutions on LB (recipient titer) and M9 medium (transformant titer). In some experiments, rifampicin was added to the M9 medium (no difference in transformation frequency was observed). The plates were incubated at 30 °C for 16 h (LB) or 40 h (M9), and recipient and transformant titers calculated from the colony-forming units. Transformation frequencies were calculated as transformants per recipient unless explicitly calculated as transformants per marker-containing DNA molecule (transformation efficiency). Mutational backgrounds in competent cells were determined in transformation assays with dialysis buffer without donor DNA. When determining transformants per marker-containing molecule, the mutational background was subtracted from the calculations.

Screening for Histidine-Prototroph Transformants. To distinguish possible *hisC*::ND5$^+$ transformants from random His$^+$ mutants, isolates were screened by PCR with primers NC1-tag-r and hisC-ins-f (Table S4). Equal amounts of cells from 10 His$^+$ isolates were suspended in water (about 10^9 cells per mL in total) and used as template. The screening PCR assays consisted of 10 μL of DyNazyme II PCR Master Mix (Thermo Scientific) amended with 1 μM $MgCl_2$, about 10^6 bacterial cells (about 10^5 cells of each isolate), and 1 μM of each primer in a total volume of 20 μL. The PCR was run at 94 °C for 5 min; 31 cycles of 92 °C for 30 s, 67.5 °C for 30 s, and 72 °C for 60 s, and final extension at 72 °C for 3 min in a PTC-200 thermocycler (MJ Research). Under these conditions, spontaneous randomly picked His$^+$ mutants gave no PCR amplificate. Positive controls included the recipient-specific primer pair NC1-recip-r and hisC-ins-f, or using a "false-positive" PCR product, obtained under the conditions specified above but with annealing temperature of 60 °C instead of 67.5 °C, as template. When a PCR product was obtained in the screening PCR assays, the sequences of the *hisC* alleles from all 10 isolates were determined by DNA sequencing.

DNA Sanger Sequencing. Some results and constructed strains were verified by Sanger sequencing using the BigDye 3.1 chemistry according to the manufacturer's instructions (Applied Biosystems). A few sequencing reactions were performed by external companies (MWG-Biotech; GATC Biotech). For the identification of the *trpE27* mutation, a PCR product covering the *A. baylyi* JV28 *trpE27* allele was PCR amplified with primers trpE-up and trpE-down (1,643 bp) and sequenced with primers trpE-up, trpE-pr, trpE-re, and trpE-down, respectively. $trpE^+$ transformants were characterized by sequencing of a 400-bp PCR amplificate (primers trpE-F3 and trpE-R3) and using trpE-F2, trpE-F3, or trpE-R3 as sequencing primer.

The mammoth mtDNA ND5 region to be used as target for the double-nucleotide exchange tag of *A. baylyi* KOM218 was confirmed by sequencing PCR amplificates with primers NC1_F1 and NC1_R1 (199 bp; sequencing primer: NC1_F1) and NC1_F2 and NC1_R2 (241 bp; sequencing primer NC1_R2).

The *hisC*::′ND5i′ fragment of pKHhisC25 was PCR amplified with primers hisC-ins-f and hisC-ins-r, and the same primers were used for two respective sequencing assays. The complete *hisC*::′ND5i′ allele of KOM218 was PCR amplified with hisC-ins-f and hisC-ctrl-r (1,737 bp) and sequenced with primers hisC-ins-f, hisC-up-f, hisC-ins-r, and hisC-ctrl-r, respectively. The *hisC* alleles of His$^+$ isolates were characterized by sequencing PCR amplificates (with primers hisC-ins-f and hisC-ins-r) using hisC-ins-f or, in some cases, hisC-ins-r, as sequencing primer.

The Δ*mutS* locus of *A. baylyi* KOM171 was PCR amplified with primer mutS-up-f and mutS-down-r and sequenced with the sequencing primer mutS-down-r3.

Spontaneous Mutation Frequency Determination. The spontaneous mutation frequencies of some *A. baylyi* strains were determined to identify phenotypic mutators. Antibiotic-sensitive cultures were inoculated from a single colony in 7 mL of LB and grown overnight. The cells were washed, resuspended in 7 mL of PBS and plated on antibiotic-containing (ampicillin, 100 μg/mL; or chloramphenicol, 25 μg/mL) medium (mutant titer; 1 mL per plate) and in appropriate dilution on LB (cell titer). The plates were incubated 72 h at 30 °C, and spontaneous mutation frequencies were calculated as mutant titer per cell titer.

Whole-Genome Analysis: Double-Nucleotide Polymorphisms in Complete Genomes from Transformable and Nontransformable Bacterial Clades. ***Multiple alignments.*** Complete genomes from transformable and nontransformable bacterial species were chosen to determine if double-nucleotide polymorphisms (DNPs) have an increased presence in multiple genome alignments within each transformable species compared with each one of the nontransformable ones. See Fig. 4*C* and Table S2 for genome sequences used. MAUVE (26) was used to perform separate whole-genome multiple alignments within each bacterial species.

Each multiple alignment was inspected for its polymorphism composition. From the total number of polymorphisms in each alignment, the proportion of mismatches involved in single, double, triple, quadruple, quintuple, and sextuple polymorphisms was computed. Only unique polymorphisms within each multiple alignment were counted. A DNP is defined as two and a "multiple" as three, four, five, or six directly adjacent polymorphisms in the alignment. A polymorphism was restricted to an alignment between two nonambiguous bases. Also, an alignment of a nonambiguous base in one sequence to a gap in the other sequence was not included in this calculation. The total absolute counts of polymorphisms are given by category in Fig. 4*D*. Species- and strain-specific counts are given in Table S2.

Statistical Analyses of the Raw Polymorphism Category Distributions, by Clade Categories. Three χ^2 tests of homogeneity were run to test whether the total counts of DNPs and the total counts of SNPs and multiples were distributed homogeneously across transformable and nontransformable species (Fig. 4 *D* and *E*). Three 2×2 contingency tables of absolute polymorphism counts were built: SNPs vs. DNPs, SNPs vs. Multiples, and DNPs vs. Multiples in transformable and nontransformable bacteria. The χ^2 test compares the observed counts in each cell of a given contingency table to the expected value for that cell. The expected value in each cell is calculated based on the margins of the contingency table that correspond to that cell. From these comparisons, the χ^2 statistic is obtained. Then a P value is calculated, in a χ^2 distribution with 1 degree of freedom, as the probability of finding a χ^2 statistic at least as extreme as the one that was found in the test. The χ^2 test show that there is a significant difference across transformable and nontransformable species between the tested polymorphism categories, with the following pattern: The SNP category has a greater proportion in the nontransformable species, as opposed to the DNP category, which has a higher proportion in the transformable species (χ^2 test, P value $<<$ 0.001). The multiples category has a higher proportion over the DNP category in the nontransformable species (χ^2 test, P value $<<$ 0.001). These χ^2 tests support an increased ratio of DNPs in transformable bacterial species. It could be that, like DNPs, the multiples category would also be increased over SNPs in transformable species; however, we find the opposite (χ^2 test, P value $<<$ 0.001). To allow direct visual comparison of the counts in Fig. 4*E*, then the y axis has been normalized to show the proportion of total polymorphism counts of DNPs, multiples, and SNPs within nontransformable and transformable species, respectively. As the columns represent absolute counts, then no error bars can be given; either a polymorphism was counted or not. Statistical analyses, plots, and data treatment were performed using custom R version 3.0.1 (27) scripts.

Genome Resequencing. To test whether differences in laboratory handling, sequencing chemistry, and genome assembly method could somehow cause the pattern we observed in our genome comparisons, we acquired genomic DNA from 25 (Table S2) of the 91 bacterial strains in our full-genome analysis and resequenced them in one batch to ensure uniform handling and data processing.

DNA samples were acquired from the publishers of the original genome sequences (Table S3). All samples were fragmented using a COVARIS sonicator set for maximum fragment length at 300 bp and 200–400 bp purified for library build. Each sample was given its own library index and then sequenced in the same lane with a 100-bp paired-end run in an Illumina HiSEq. 2000 with version 3 chemistry and CASAVA-1.8.2.

Sequencing adapters were trimmed from the reads using a custom Python script, the reads were subsequently trimmed from 3′ to a quality score of 20, and reads with average quality less than 20 or containing Ns were discarded. On average, 97.2% of the reads passed trimming and quality control. Hereafter, the reads were mapped using bwa-0.5.9 (28) to the respective reference genomes, the alignments were sorted and filtered to minimum mapping quality of 30 using samtools (29), and duplicates were removed using Picard MarkDuplicates (http://picard.sourceforge.net/). SNPs and indels were called using samtools mpileup and bcftools and filtered using vcfutils.pl (29). In addition, the variants were filtered to minimum 10× depth and posterior probability of 0.001. Consensus sequences were created using samtools mpileup, bcfutils and vcfutils.pl vcf2fq, and all heterozygote variant positions were converted to reference bases (Table S3). The sequence data were submitted to the European Nucleotide Archive under accession number PRJEB4698 and are available at www.ebi.ac.uk/ena/data/view/PRJEB4698.

Calculation of How Much Old DNA Is Released from Soil and Sediments Each Year. The yearly amount of sediment that rivers discharge into the oceans has been estimated to 12,610 ± 15% megaton/y (30). Various determinations of extracellular DNA in soil and sediments yield an average range from around 80 to >1,000 ng/g dry matter (31). That is, for 80 ng DNA/g: 1.261×10^4 megaton $\times\ 10^{12}$ g/megaton $\times\ 8 \times 10^{-8}$ g DNA/g = 1.01×10^9 g DNA/y = 1,010 ± 151 ton DNA/y. In addition, for 1,000 ng DNA/g: 1.261×10^4 megaton $\times\ 10^{12}$ g/megaton $\times\ 10^{-6}$ g DNA/g = 1.261×10^{10} g DNA/y = 12,610 ± 1,890 ton DNA/y. This gives a range of 859–14,500 ton DNA/y. The estimate of sediment discharge does not include permafrost degradation, which is expected to be a major future contribution.

1. de Vries J, Heine M, Harms K, Wackernagel W (2003) Spread of recombinant DNA by roots and pollen of transgenic potato plants, identified by highly specific biomonitoring using natural transformation of an *Acinetobacter* sp. *Appl Environ Microbiol* 69(8):4455–4462.
2. Sawula RV, Crawford IP (1972) Mapping of the tryptophan genes of *Acinetobacter calcoaceticus* by transformation. *J Bacteriol* 112(2):797–805.
3. Dutra BE, Sutera VA, Jr., Lovett ST (2007) RecA-independent recombination is efficient but limited by exonucleases. *Proc Natl Acad Sci USA* 104(1):216–221.
4. Bryan A, Swanson MS (2011) Oligonucleotides stimulate genomic alterations of *Legionella pneumophila*. *Mol Microbiol* 80(1):231–247.
5. Harms K, Schön V, Kickstein E, Wackernagel W (2007) The RecJ DNase strongly suppresses genomic integration of short but not long foreign DNA fragments by homology-facilitated illegitimate recombination during transformation of *Acinetobacter baylyi*. *Mol Microbiol* 64 (3):691–702.
6. Kickstein E, Harms K, Wackernagel W (2007) Deletions of *recBCD* or *recD* influence genetic transformation differently and are lethal together with a *recJ* deletion in *Acinetobacter baylyi*. *Microbiology* 153(Pt 7):2259–2270.
7. Altschul SF, Gish W, Miller W, Myers EW, Lipman DJ (1990) Basic local alignment search tool. *J Mol Biol* 215(3):403–410.

8. Barbe V, et al. (2004) Unique features revealed by the genome sequence of *Acinetobacter* sp. ADP1, a versatile and naturally transformation competent bacterium. *Nucleic Acids Res* 32(19):5766–5779.
9. Burdett V, Baitinger C, Viswanathan M, Lovett ST, Modrich P (2001) In vivo requirement for RecJ, ExoVII, ExoI, and ExoX in methyl-directed mismatch repair. *Proc Natl Acad Sci USA* 98(12):6765–6770.
10. Thoms B, Borchers I, Wackernagel W (2008) Effects of single-strand DNases ExoI, RecJ, ExoVII, and SbcCD on homologous recombination of *recBCD*$^+$ strains of *Escherichia coli* and roles of SbcB15 and XonA2 ExoI mutant enzymes. *J Bacteriol* 190(1):179–192.
11. Dahlmann HA, Vaidyanathan VG, Sturla SJ (2009) Investigating the biochemical impact of DNA damage with structure-based probes: Abasic sites, photodimers, alkylation adducts, and oxidative lesions. *Biochemistry* 48(40):9347–9359.
12. Seeberg E, Eide L, Bjørås M (1995) The base excision repair pathway. *Trends Biochem Sci* 20(10):391–397.
13. Römpler H, et al. (2006) Nuclear gene indicates coat-color polymorphism in mammoths. *Science* 313(5783):62.
14. de Vries J, Wackernagel W (2002) Integration of foreign DNA during natural transformation of *Acinetobacter* sp. by homology-facilitated illegitimate recombination. *Proc Natl Acad Sci USA* 99(4):2094–2099.
15. Metzgar D, et al. (2004) *Acinetobacter* sp. ADP1: An ideal model organism for genetic analysis and genome engineering. *Nucleic Acids Res* 32(19):5780–5790.
16. Friedrich A, Hartsch T, Averhoff B (2001) Natural transformation in mesophilic and thermophilic bacteria: Identification and characterization of novel, closely related competence genes in *Acinetobacter* sp. strain BD413 and *Thermus thermophilus* HB27. *Appl Environ Microbiol* 67(7):3140–3148.
17. Claverys JP, Lacks SA (1986) Heteroduplex deoxyribonucleic acid base mismatch repair in bacteria. *Microbiol Rev* 50(2):133–165.
18. Kunkel TA, Erie DA (2005) DNA mismatch repair. *Annu Rev Biochem* 74:681–710.
19. Iyer RR, Pluciennik A, Burdett V, Modrich PL (2006) DNA mismatch repair: Functions and mechanisms. *Chem Rev* 106(2):302–323.
20. Harms K, Wackernagel W (2008) The RecBCD and SbcCD DNases suppress homology-facilitated illegitimate recombination during natural transformation of *Acinetobacter baylyi*. *Microbiology* 154(Pt 8):2437–2445.
21. Keen NT, Tamaki S, Kobayashi D, Trollinger D (1988) Improved broad-host range plasmids for DNA cloning in Gram-negative bacteria. *Gene* 70(1):191–197.
22. Bacher JM, Metzgar D, de Crécy-Lagard V (2006) Rapid evolution of diminished transformability in *Acinetobacter baylyi*. *J Bacteriol* 188(24):8534–8542.
23. Sambrook J, Fritsch EF, Maniatis T (1989) *Molecular Cloning: A Laboratory Manual* (Cold Spring Harbor Lab Press, Cold Spring Harbor, NY).
24. Hanahan D (1983) Studies on transformation of *Escherichia coli* with plasmids. *J Mol Biol* 166(4):557–580.
25. Romanowski G, Lorenz MG, Wackernagel W (1993) Use of polymerase chain reaction and electroporation of *Escherichia coli* to monitor the persistence of extracellular plasmid DNA introduced into natural soils. *Appl Environ Microbiol* 59(10):3438–3446.
26. Darling AE, Mau B, Perna NT (2010) progressiveMauve: Multiple genome alignment with gene gain, loss and rearrangement. *PLoS One* 5(6):e11147.
27. R Core Team (2013) R: A language and environment for statistical computing. (R Foundation for Statistical Computing, Vienna, Austria). Available at www.R-project.org. Version 3.0.1.
28. Li H, Durbin R (2009) Fast and accurate short read alignment with Burrows-Wheeler transform. *Bioinformatics* 25(14):1754–1760.
29. Li H, et al. (2009) The Sequence Alignment/Map format and SAMtools. *Bioinformatics* 25(16):2078–2079.
30. Syvitski JPM, Vörösmarty CJ, Kettner AJ, Green P (2005) Impact of humans on the flux of terrestrial sediment to the global coastal ocean. *Science* 308(5720):376–380.
31. Pietramellara G, Ascher J, Borgogni F, Ceccherini GGMT, Nannipieri P (2009) Extracellular DNA in soil and sediment: Fate and ecological relevance. *Biol Fertil Soils* 45(3):219–235.

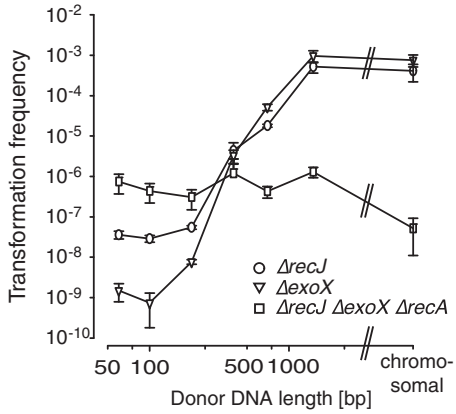

Fig. S1. Natural transformation of ss-exonuclease- and RecA-deficient mutants. Transformation frequencies (means with SDs from three or more experiments) obtained with 100 ng/mL donor DNA of different lengths and calculated as transformants per recipient as in Fig. 1*C*. Δ*recJ* (circles; $n = 3$), Δ*exoX* (triangles; $n = 3$), and Δ*recJ* Δ*exoX* Δ*recA* (squares; $n = 3$–4).

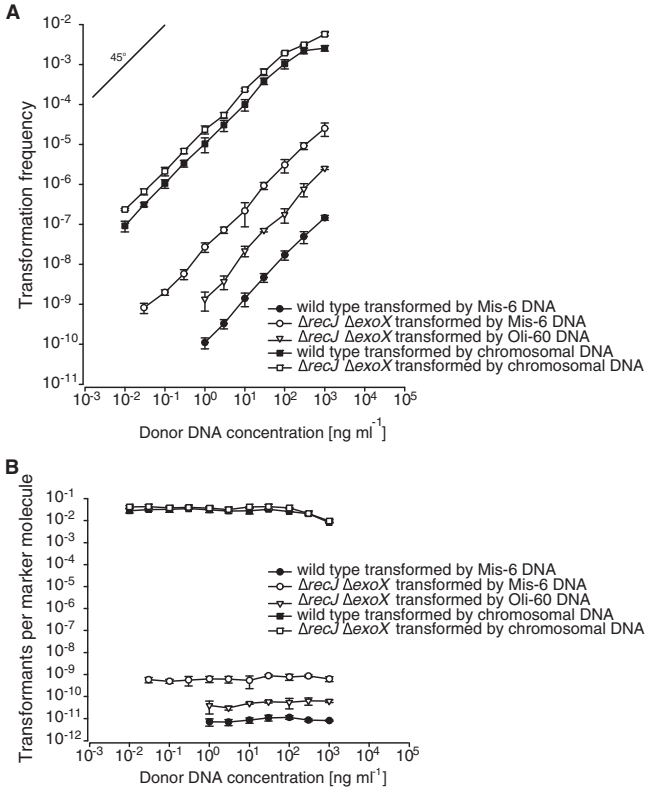

Fig. S2. Natural transformation of *A. baylyi* by different donor DNA concentrations. Natural transformation frequencies of the wild-type (filled symbols) and Δ*recJ* Δ*exoX* (open symbols) strains with different donor DNA substrates (Mis-6: circles; Oli-60: triangles; chromosomal DNA: squares) at various concentrations. (*A*) Transformation frequency given as transformants per recipient cell, calculated as in Fig. 1*C*. (*B*) Transformation efficiency given as transformants per marker-containing donor DNA molecule. The mutational background (obtained in control experiments without DNA) has been subtracted from the results.

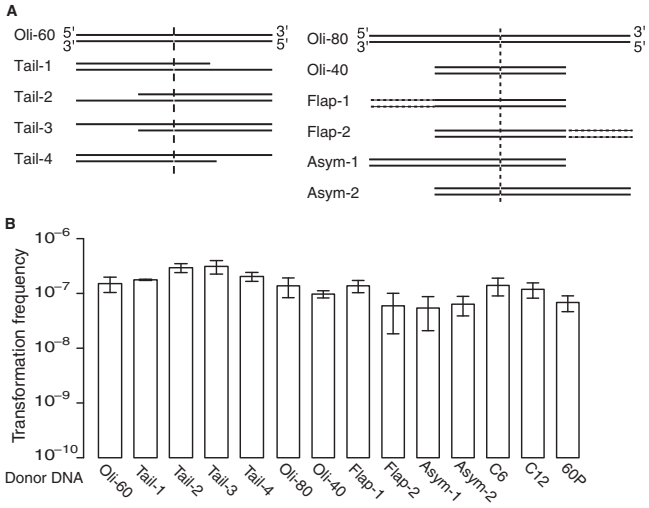

Fig. S3. Natural transformation by DNA substrates with terminal modifications. (*A*) Schematic proportional sizes of donor DNA substrates. Orientations and marker positions are the same as in Fig. 2*A*. Dashed line extensions indicate heterologous DNA. (*B*) Transformation frequencies of the Δ*recJ* Δ*exoX* strain by donor DNA substrates mentioned in the text or shown in *A* (from $n = 3$–7 experiments, for Oli-60: $n = 26$). Transformation frequencies were determined as in Fig. 1*C*.

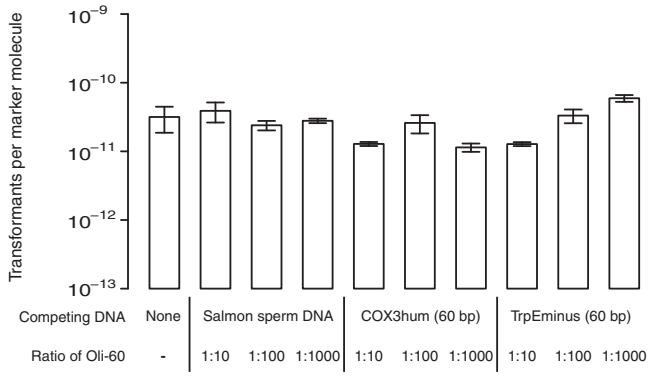

Fig. S4. Natural transformation in the presence of excess of competing DNA. Transformation efficiency of the Δ*recJ* Δ*exoX* strain calculated as transformants per marker molecule for the Oli-60 substrate without and with competing nontransforming DNA in 10-, 100-, and 1,000-fold excess. For Oli-60 without competing DNA, data from experiments with different donor DNA concentrations (1 ng/mL; 10 ng/mL; 100 ng/mL) were pooled ($n = 15$). For experiments with the different competing DNA substrates, the concentrations were as follows: for the 1:10 ratio, 100 ng/mL Oli-60 and 900 ng/mL competing DNA; for the 1:100 ratio, 10 ng/mL Oli-60 and 990 ng/mL competing DNA; for the 1:1,000 ratio, 1 ng/mL Oli-60 and 999 ng/mL competing DNA ($n = 3$ for each experiment); for salmon sperm DNA, experiments were also conducted with 10 ng/mL Oli-60 plus 90 ng/mL salmon sperm DNA ($n = 3$) for the 1:10 ratio, and the data were pooled. Maximal total DNA concentration was 1 μg/mL to avoid saturation of DNA uptake capacity.

Other Supporting Information Files

Table S1 (DOCX)
Table S2 (DOCX)
Table S3 (DOCX)
Table S4 (DOCX)
Table S5 (DOCX)